

## Mechanical Properties of Polymer Gels with Controlled Network Structure

(精密網目構造を有するポリマーゲルの力学特性)

赤木 友紀

**【Introduction】** Hydrogels have attracted great attention due to the new application such as soft and wet materials and cell scaffolds. However, it is difficult to control and predict the mechanical properties of hydrogels. One of the main reasons for this difficulty is structural inhomogeneity inherently introduced into the polymer network during the crosslinking process. The inhomogeneities cause the disagreement between the theoretical prediction and real data.

Recently, as a new class of polymer network, we have designed and fabricated Tetra-PEG gel<sup>1</sup>. Tetra-PEG gel is formed from A-B type cross-end coupling of two tetra-arm PEG prepolymers of the same size (Tetra-PEG modules). In the SANS measurement, the excess scattering was not obtained in the region below 200 nm, suggesting an extremely homogeneous network structure of Tetra-PEG gel.<sup>2</sup>

In this study, we fabricated Tetra-PEG gel with the different prepolymer size. Using these gels, we evaluated the mechanical properties. First, we measured the reaction efficiency. Second, we evaluated the mechanical property in the small deformation region. Third, we performed the tearing test and evaluated the fracture energy. Finally, we evaluated the mechanical property in the large deformation region.

**【Experimental】** *Synthesis of prepolymers:* Tetra-amine-terminated PEG (TetraPEG-NH<sub>2</sub>) and tetra-NHS-glutarate-terminated PEG

(TetraPEG-OSu) were prepared from tetrahydroxyl-terminated PEG (TetraPEG) having equal arm lengths. The molecular weights ( $M_p$ ) of TetraPEG-NH<sub>2</sub> and TetraPEG-OSu were matched to each other ( $M_p = 5, 10, 20, 40$  kg/mol).

*Fabrication of Tetra-PEG gels:* Constant amounts of TetraPEG-NH<sub>2</sub> and TetraPEG-OSu ( $\phi$ : 0.034 ~ 0.096) were dissolved in phosphate buffer (pH7.4) and phosphate-citric acid buffer (pH5.8), respectively. In order to control the reaction rate, the ionic strengths of the buffers were adjusted. Two solutions were mixed, and the resulting solution was poured into the mold. At least 12 hours were allowed for the completion of the reaction before the following experiment was performed. *FT-IR measurement:* The gels were prepared as rectangular films (height: 20 mm, width: 20 mm, thickness: 10 mm). Prepared gel samples were soaked in H<sub>2</sub>O for 2 days at room temperature and then dried. The dried samples were cut into thin films (thickness: 40  $\mu$ m). First, these samples were soaked in D<sub>2</sub>O, then soaked in a mixture solvent of D<sub>2</sub>O and PEG ( $M_w = 0.40$  kg/mol) with volume ratio of 1:1. *Stretching measurement:* The stretching measurement was carried out on dumbbell shaped specimens at a constant velocity of 60 mm/min. The gel samples were used in an as-prepared state. *Tearing test:* The gels were cut using a gel cutting machine (50 mm  $\times$  7.5 mm  $\times$  1 mm, with an initial notch of 20 mm). The two arms of the test sample were clamped and one arm was pulled upward at a

constant velocity of 40 mm/min, while the other arm was maintained stationary.

**【Results and Discussion】 Small deformation:**

The reaction efficiency ( $p$ ) was directly estimated by FT-IR measurement.  $p$  was in the range 0.82–0.95 in 5k, 10k and 20k Tetra-PEG gels.<sup>3,4</sup> In contrast,  $p$  was between 0.70–0.81 in 40k Tetra-PEG gel. The decrease in  $p$  may be caused by the decrease of the reaction rate with increase in molecular weight. We compared the elastic modulus ( $G$ ) measured by a stretching measurement, and that predicted from  $p$  using affine ( $G_{af}$ ) and phantom ( $G_{ph}$ ) network models. Using the tree-like approximation, the number densities of elastically effective chains ( $\nu$ ) and active crosslinks ( $\mu$ ) for tetra-functional network is predicted as,

$$\nu = M_{pre} \left\{ \frac{3}{2} \cdot \frac{3}{4} C_3 (1 - P_\infty)^3 P_\infty + \frac{4}{2} \cdot \frac{4}{4} C_4 (1 - P_\infty)^4 \right\}$$

$$\nu - \mu = M_{pre} \left\{ \frac{1}{3} \cdot \frac{3}{2} \cdot \frac{3}{4} C_3 (1 - P_\infty)^3 P_\infty + \frac{1}{2} \cdot \frac{4}{2} \cdot \frac{4}{4} C_4 (1 - P_\infty)^4 \right\}$$

, where  $M_{pre}$  is the number density of the Tetra-PEG prepolymers. The affine and phantom network models predict the elastic modulus as,

$$G_{af} = \nu RT$$

$$G_{ph} = (\nu - \mu) RT$$

,where  $R$  is the gas constant and  $T$  is the absolute temperature. The variation of  $G$ ,  $G_{af}$  and  $G_{ph}$  against  $\phi_0$  of Tetra-PEG gel (10k and 40k) is shown in Figure 1. As for the 10k and 20k Tetra-PEG gels,  $G_{ph}$  and  $G$  corresponded well with each other in a wider range than the other gels, suggesting that their elasticities is roughly predicted by the phantom network model. As for the 5k Tetra-PEG gel, the downward deviation of  $G$  from  $G_{ph}$  was increasingly pronounced with decreasing  $\phi_0$ . On the other hand, the Tetra-PEG

gel (40k) shows distinct behavior;  $G$  was above  $G_{ph}$  and near  $G_{af}$ .

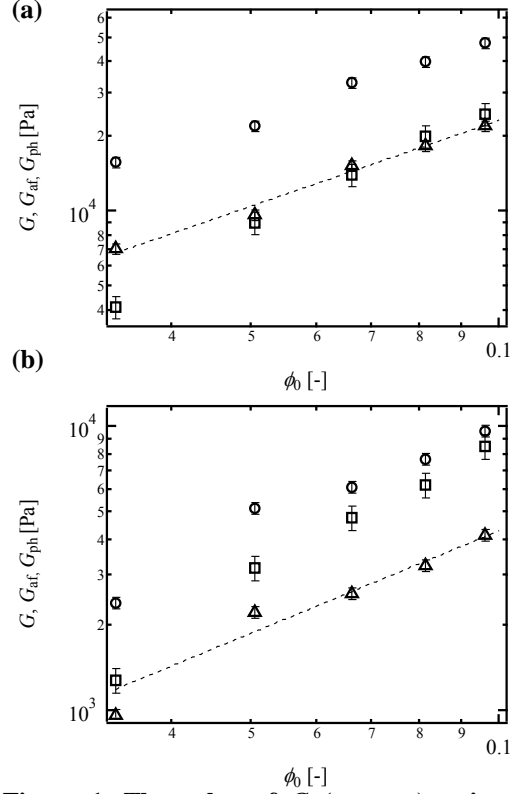


**Figure 1.** The value of  $G$  (squares) estimated from the stretching measurement,  $G_{af}$  (circles) and  $G_{ph}$  (triangles), estimated from the reaction efficiency ( $p$ ) as a function of  $\phi_0$  in (a) 10k and (b) 40k Tetra-PEG gel.

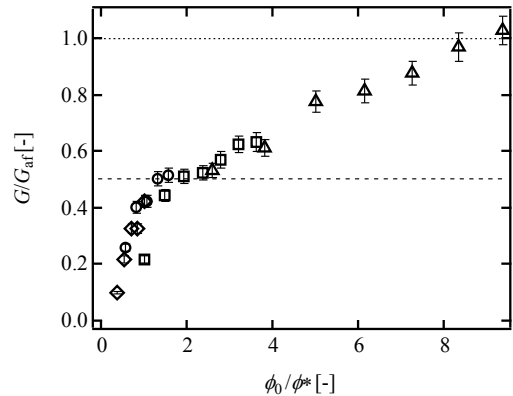


**Figure 2.** The value of  $G/G_{af}$  as a function of  $\phi_0/\phi^*$  in Tetra-PEG gel (5k, rhombus; 10k, circle; 20k, square; 40k, triangle).

In order to discuss the whole tendency,  $G/G_{af}$  was plotted against  $\phi_0/\phi$  (Figure 2). In this figure, phantom and affine network model predictions were the flat lines showing  $G/G_{af} = 0.5$  (dashed line) and 1 (dotted line), respectively. All of the data fall onto a single curve. In the range from  $\phi$  to  $3.0\phi$ , the elastic moduli were well predicted by the phantom network model. The downward deviation below  $\phi$  is due to the formation of elastically ineffective loops. In the range above  $3.0\phi$ ,  $G/G_{af}$  increased with increasing  $\phi_0$  and approached to 1.0. This data strongly suggests that trapped entanglements are introduced to the network or that the model shifts to the affine network model, or both in the region above  $3.0\phi$ . Only from these results, we cannot distinguish whether the deviation from the phantom network model prediction is originated from trapped entanglements or from the change in models. Thus, we investigate the trapped entanglements by the tearing measurement.

**Tearing measurement:** In the Lake-Thomas model, the fracture energy is estimated as the energy needed to break the chemical bonds on the fracture surface. According to the model,  $T_0$  is represented as,

$$T_0 = \frac{1}{2} L \nu N U.$$

, where  $L$  is the displacement length and  $U$  is the energy required to rupture a monomer unit. Assuming the network structure is formed only by chemical crosslinks and there is no trapped entanglements,  $\nu$  and  $L$  are represented as follows,

$$\nu \sim \frac{\phi_0}{N}$$

$$L \sim a N^{1/2}$$

, where  $a$  is the monomer length. Thus,  $T_0$  scales with the  $\phi_0$  and  $N$  as

$$T_0 \sim \phi_0 N^{1/2}.$$

This agreement indicates that the assumptions on  $\nu$  and  $L$  are valid, i.e., there is no trapped entanglement regardless of  $\phi_0$  and  $N$ .

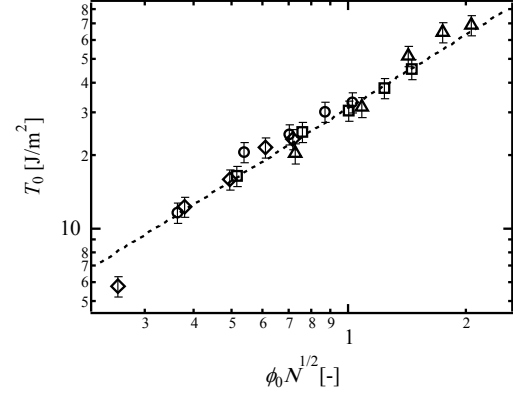


**Figure 3. Fracture energy as a function of  $\phi_0 N^{1/2}$  (5k, rhombus; 10k, circle; 20k, square; 40k, triangle).**

We plotted the all the data of  $T_0$  against  $\phi_0 N^{1/2}$  (Figure 4). As expected, all the data fell onto a master curve showing the relationship,  $T_0 \sim \phi_0 N^{1/2}$ . These data indicated that there are few trapped entanglements. Taking into account these data, it is strongly suggested that the model predicting the elastic modulus shifts model with increasing  $\phi$  and  $N$ .

**Large deformation:** In order to calculate the maximum deformation of Tetra-PEG gel, we utilized the extended Gent model. In the extended Gent model, the relationship of stress ( $\sigma$ ) and elongation ratio ( $\lambda$ ) is represented as follows.

$$\sigma = \frac{C_1 (\lambda - \lambda^{-2})}{\left(1 - \frac{\lambda^2 + 2\lambda^{-1} - 3}{\lambda_{\max}^2 + 2\lambda_{\max}^{-1} - 3}\right)} + C_2 (1 - \lambda^{-3})$$

, where  $\lambda_{\max}$  is the ultimate deformation ratio of network strands under uniaxial stretching. The stress-elongation curves of Tetra-PEG gel were well predicted by this model.  $\lambda_{\max}$  increased with increasing  $\phi$ , showing the relationship,  $\lambda_{\max} \sim \phi_0^{1/3}$ .

In the Kuhn model,  $\lambda_{\max}$  is estimated as the ratio of the contour length ( $L$ ) to the root-mean-square end-to-end distance ( $R_g$ ) of network strands:

$$\lambda_{\max} = \frac{L}{R_g} = \frac{aN}{aN^{1/2}} \approx N^{1/2}$$

This model cannot predict the  $\phi_0$  dependence of  $\lambda_{\max}$  observed in Tetra-PEG gel. Here, we propose a new model predicting the ultimate elongation ratio of polymer gels.

In the Kuhn model,  $\lambda_{\max}$  is estimated as the ratio of the  $L$  to the  $R_g$  of network strands. Because the contour length in the numerator has distinct molecular picture associated with the breakage, the denominator may be wrong. Thus, we set the unknown,  $d$ , as a denominator and investigate the form of  $d$  in comparison with the experimental results.

$$\lambda_{\max} = \frac{aN}{d} \sim \phi_0^{0.3} N^{0.7}$$

By solving this equation for  $d$ , we obtained

$$d \sim \left( \frac{\phi_0}{N} \right)^{-0.3}$$

In tearing measurement, it is revealed that Tetra-PEG gel has few trapped entanglements and that  $\nu$  scales with  $\phi_0$  and  $N$  as,  $\nu \sim \phi_0/N$ . By substituting  $\nu$ , we obtain the relationship,  $d \sim \nu^{-0.3}$ . The power similar to  $-1/3$  suggests that  $d$  has the same power law as that of the simple geometrical distance between the nearest prepolymers. If  $d$  is modeled as above mentioned,  $\lambda_{\max}$  is given by,

$$\lambda_{\max} = \frac{aN}{d} \sim \frac{aN}{(N/\phi_0)^{1/3}} \sim N^{2/3} \phi_0^{1/3}$$

We replotted the all the data of  $\lambda_{\max}$  against  $N^{2/3} \phi_0^{1/3}$  in Figure 4. As expected, all the data fall onto a master curve showing the relationship,  $\lambda_{\max} \sim N^{2/3} \phi_0^{1/3}$ .

### 【Conclusion】

The results of this study are summarized as follows.

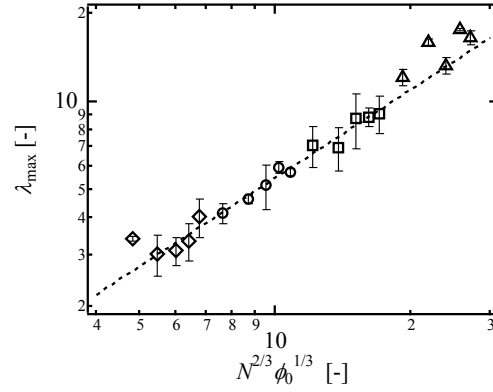


**Figure 4. Maximum deformation as a function of  $N^{2/3} \phi_0^{1/3}$  in Tetra-PEG gel. (5k, rhombus; 10k, circle; 20k, square; 40k, triangle). The dashed line is the master curve.**

The fracture energy of Tetra-PEG gel was explained by the Lake-Thomas model, suggesting that only few trapped entanglements exist in the network structure. The model predicting the elastic modulus shifts from the phantom network model to the affine network model at around the overlapping polymer concentration. From evaluation of the ultimate elongation ratio, it is suggested that  $\lambda_{\max}$  did not obey the Kuhn model, but obeyed our new semi-empirical model.

It is strongly suggested that Tetra-PEG gel has ideally homogeneous network structure. Through the investigation on Tetra-PEG gel, the models predicting the contribution of chemical crosslink to the mechanical properties of polymer gels were clarified.

### 【Reference】

- 1) Sakai, T.; Matsunaga, T. *Macromolecules* **2009**, 42, 1344-1351.
- 2) Matsunaga, T.; Sakai, T. *Macromolecules* **2009**, 42, 1344-135
- 3) Akagi Yuki, Matsunaga, T. *Macromolecules* **2010**, 43, 488-493
- 4) Akagi Yuki, Katashima, T. *Macromolecules* **2011**, 44, (4), 5817-5821